Exploiting Spectrum Access Ability for Cooperative Spectrum Harvesting

Chao Ren, *Member, IEEE*, Haijun Zhang, *Senior Member, IEEE*, Jian Chen, *Member, IEEE*, and Chintha Tellambura, *Fellow, IEEE*

***Abstract*— Spectrum harvesting is needed for large-scale wireless networks to access underutilized spectrum and support multiple heterogeneous users. Cooperative spectrum harvesting (CSH) allows for improved co-channel existence and intra-/inter-cell interference mitigation, which dramatically improves spectral efficiency. However, good performance metrics to quantify CSH schemes are not available. For example, existing metrics such as data rate, error/outage probability, and multiplexing/diversity gains may not clearly distinguish large signal-to-interference-plus-noise ratio (SINR) scenarios and sum-rate performance for multiple links. To overcome these limitations, we propose two new metrics called spectrum access level (SAL) and user participation level (UPL). The advantages of these metrics are: 1) achieving distinct upper bounds for multiple links; 2) upper bounds being evaluated directly by basic CSH system model; and 3) determining the performance at any power level of CSH schemes even if they are not interference exempt. Moreover, a novel CSH system model is conceived to achieve satisfying spectrum access ability based on SAL and UPL, and an interference-exempt scheme is designed to achieve relevant upper bounds. Numerical results verify the efficiency of SAL and UPL, and the spectrum access ability of proposed system model with interference-exempt scheme.**

***Index Terms*— Spectrum harvesting, spectrum sharing, cooperative communications, signal space diversity, interference cancellation.**

Manuscript received December 10, 2017; revised June 24, 2018 and September 25, 2018; accepted November 3, 2018. Date of publication November 14, 2018; date of current version March 15, 2019. This work is supported by the National Natural Science Foundation of China (61822104, 61471025, 61771044), the Young Elite Scientist Sponsorship Program by CAST (2016QNRC001), the Research Foundation of Ministry of Education of China & China Mobile (MCM20170108), Beijing Natural Science Foundation (L172025, L172049), 111 Project (No. B170003), the China Postdoctoral Science Foundation (2018M630072), and the Fundamental Research Funds for the Central Universities (FRF-GF-17-A6, RC1631, FRF-TP-18-015A1). The associate editor coordinating the review of this paper and approving it for publication was H.-M. Wang. *(Corresponding author: Haijun Zhang.)*

C. Ren and H. Zhang are with the Beijing Advanced Innovation Center for Materials Genome Engineering, University of Science and Technology Beijing, Beijing 100083, China, with the Beijing Engineering and Technology Research Center for Convergence Networks and Ubiquitous Services, University of Science and Technology Beijing, Beijing 100083, China, and also with the Institute of Artificial Intelligence, University of Science and Technology Beijing, Beijing 100083, China (e-mail: chaoren@ustb.edu.cn; haijunzhang@ieee.org).

J. Chen is with the State Key Laboratory of Integrated Services Networks, Xidian University, Xi'an 710071, China (e-mail: jianchen@mail.xidian.edu.cn).

C. Tellambura is with the Department of Electrical and Computer Engineering, University of Alberta, Edmonton, AB T6G 2V4, Canada (e-mail: chintha@ece.ualberta.ca).

Digital Object Identifier 10.1109/TCOMM.2018.2881259

I. Introduction

FUTURE wireless networks (fifth generation (5G) and beyond) must support tremendous numbers of high-rate data-hungry mobile applications, such as online virtual reality, social media services, 4K-resolution video streaming and others. Thus, these networks must improve, compared to previous wireless generations, spectral efficiency by ten fold and cut the costs by 100 fold or more [1], [2]. However, because these network will employ heterogeneity, dense device deployment and experience massive interference, spectrum scarcity emerges as a key bottleneck to satisfy the rapidly increasing spectrum demands on congested spectral bands. Hence improving the potential capacity and reducing outage by harvesting the limited spectral resource are both crucial challenges and opportunities.

A. From Spectrum Harvesting to Cooperative Spectrum Harvesting

Spectrum harvesting involves a collection of advanced technologies that can efficiently harvest the underutilized spectrum, which includes spectrum sensing, spectrum management and spectrum sharing [3]–[8].

Different from the other two approaches, spectrum sharing particularly emphasizes on performance guarantee for both primary and secondary sides in underlay networking, spectrum trading [9] and spectrum leasing [10] scenarios. Among these specific scenarios, spectrum trading and spectrum leasing are also known as strategies for *cooperative spectrum sharing* [11], which are designed based on mutually beneficial exchange, such as the exchange in spectrum trading (i.e., price $\overset{\text{spectrum}}{\underset{\text{trading}}{\longleftrightarrow}}$ demand) and the mutual benefit in spectrum leasing (i.e., exclusive transmission phase $\overset{\text{spectrum}}{\underset{\text{leasing}}{\longleftrightarrow}}$ relaying benefits). Since spectrum leasing necessitates that the secondary users (SUs) offer their aid in primary transmissions instead of monetary payment, it may be more suitable for implementing cost-efficient secondary access with full cooperation between PUs and SUs.

Likewise, to more efficiently harvest the underutilized spectrum and incentivize win-win spectral coexistence, the paradigm of *cooperative spectrum harvesting* (CSH) [12] can be established on a basis of collaborative co-channel access, full multi-user cooperation and advanced interference mitigation technologies. In CSH, SUs relay primary data and improve

TABLE I
KEY FEATURES OF SPECTRUM LEASING AND CSH

strategy	SU function	offering from PUs	interference type
spectrum leasing	relaying PUs' data in two phases	allowance for SUs' transmission in an exclusive third phase	PU $\rightleftarrows$ PU, SU $\rightleftarrows$ SU
CSH	relaying PUs' data in two phases	allowance for SUs' transmission in PUs' relaying phases	PU $\rightleftarrows$ PU, SU $\rightleftarrows$ SU SU $\rightleftarrows$ PU

the performance of primary user (PU) and, in return, obtain spectrum access opportunities [13]–[22]. Although the key features of CSH seem similar to spectrum leasing (Table I), CSH may have distinct advantages in compressing the secondary transmission phase into primary relaying phases and letting multiple SUs and PUs access the same spectral resources simultaneously, and is thus believed to offer a cost-effective and spectral efficient perspective in exploiting spectrum access ability [12], [23]–[25].

Zhai *et al.* [17], Pei and Liang [18], Ma *et al.* [19], and Duan *et al.* [26] proposed fundamental schemes for CSH, where the essence and fundamental approach is spectrum access regarding co-channel interference (Table I). Moreover, to provide more efficient spectrum utilization, it is also beneficial if we overcome the half-duplex time efficiency loss incurred by SU's relaying. Performance evaluation is critical for good characterization and improvement of CSH systems, and the advantages, drawbacks and special features of CSH should be addressed. To this end, we summarized the above-mentioned factors of system design and evaluation as main factors (F1-F5).

- **(F1): Drawback - Time Efficiency Loss.**
  Although CSH offers additional gains for primary and secondary systems, a symbol reception takes more phases. Accordingly, two kinds of time efficiency loss can be measured, which are originated from:
  1) two-hop transmission - additional hop requires an extra phase and decreases the rate (symbol/phase) (e.g. $\frac{1}{2}$ duplex loss induced by half-duplex relaying);
  2) phase underutilization - symbols of PU and SU can only be transmitted in certain phases (say T_{PU} and T_{SU} respectively) during cooperative phases T_c ($T_c = T_{\text{PU}} \cup T_{\text{SU}}$).

  We use $\mathcal{D}_*$ and $\mathcal{P}_*$ ($* \in \{\text{PU}, \text{SU}\}$) to represent the two factors of time efficiency loss respectively, where $0 < \mathcal{D}_* \leq 1$ and $0 \leq \mathcal{P}_* = \frac{|T_*|}{|T_c|} \leq 1$. Then, the time efficiency loss for user $*$ can be evaluated by $\tau_* = \mathcal{P}_* \times \mathcal{D}_*$. For instance, in a three-phase CSH scheme [26], primary symbols are transmitted in the first two phases ($|T_{\text{PU}}| = 2$), and SUs[1] obtain access permission only in the third phase ($|T_{\text{SU}}| = 1$), resulting in $\mathcal{P}_{\text{PU}} = \frac{|T_{\text{PU}}|}{|T_c|} = \frac{2}{3}$ and $\mathcal{P}_{\text{SU}} = \frac{|T_{\text{SU}}|}{|T_c|} = \frac{1}{3}$. It is straightforward to derive that $\mathcal{D}_{\text{PU}} = \frac{1}{2}$, $\mathcal{D}_{\text{SU}} = 1$, $\tau_{\text{PU}} = \frac{1}{3}$ and $\tau_{\text{SU}} = \frac{1}{3}$.
- **(F2): Drawback - Excessive Interference.**
  To recover the time efficiency loss (F1), some CSH schemes may maximally overlap the transmission phases for PUs and SUs, i.e. $T_{\text{PU}} = T_{\text{SU}} = T_c$ ($\mathcal{P}_* = 1$), however, resulting in severe mutual interference, say CSH interference (CSHI). CSHI can have a massive impact and impedes the ultra-dense deployment of nodes. Thus, a CSHI mitigation strategy is essential.
  To focus on the evaluation of CSHI mitigation, one may consider two conditions: 1) ignore interference from other CSH group (F3); and 2) assume infinite transmit power to examine performance bounds. Then, if a CSH strategy is successfully designed for CSHI-exemption, the SINR will be infinite; otherwise, it is limited to a floor (the rule in (F4)).
- **(F3): CSH Group with Fixed Number of Users.**
  If PUs and SUs reach an agreement for CSH strategy $\mathcal{C}$, share a fraction of primary frequency/time resource $\mathcal{FT}$, and can cooperate with each other following (F4), we define a CSH group as $\mathcal{N}_{\text{CSH}} = \mathcal{N}_{\text{PU}} \cup \mathcal{N}_{\text{SU,r}} \cup \mathcal{N}_{\text{SU,t}}$, where $\mathcal{N}_{\text{PU}}$ denotes PUs joining in $\mathcal{C}$, $\mathcal{N}_{\text{SU,r}}$ denotes SUs acting as relays for PUs in $\mathcal{N}_{\text{PU}}$, and $\mathcal{N}_{\text{SU,t}}$ denotes the SUs having permission from $\mathcal{C}$ to transmit or receive over $\mathcal{FT}$.
  One major purpose of CSH is making the number of accessed PUs and SUs over $\mathcal{FT}$ as large as possible, which is highly dependent on protocol design and CSHI mitigation on $\mathcal{C}$. If no more users can be accessed by existing CSH strategies, this 'fix number' of maximized CSH group directly reflects the ability of spectrum access for each CSH strategy. For instance, in CSH model, Pei and Liang [18] designed a protocol with at most one SUs ($|\mathcal{N}_{\text{SU,r}}| = 1$) acting as PU's relay and sharing the spectrum of two PUs ($|\mathcal{N}_{\text{PU}}| = 2$).
- **(F4): Rule - Matched Transmit Power.**
  To overcome high propagation loss, in CSH, SUs assist primary transmission [27]. To establish this user cooperation in a CSH group,[2] the transmit power levels of all nodes may follow the rule: for $\forall m \in \{1, \cdots, |\mathcal{N}_{\text{PU}}|\}$ and $\forall n \in \{1, \cdots, |\mathcal{N}_{\text{SU,r}} \cup \mathcal{N}_{\text{SU,t}}|\}$, the transmit power of m-th PU and n-th SU must satisfy $\Theta(P_{Pm}) = \Theta(P_{Sn})^3 = cP$, where P is a reference power and $c, P \in \mathbb{R}^+$. If this rule is unmatched, CSH cooperation with heterogeneous transmit power levels may not be established properly on the same channel. For instance, if $P_{pm} \propto P_{sn}^3$, the n-th SU's signal with power P_{sn} vanishes as the

[1]For simplicity, we assume only one pair of SUs exists in this model.

[2]The cooperation in overlay strategy would be established on condition that nodes follow some common rules in $\mathcal{C}$, even though they are heterogeneous. According to protocol design, rules can be chosen from: making transmit power compatible with other nodes, getting synchronization with all nodes, being aware of other nodes' codebooks and so on.

[3]Recalling Knuth's notation [28]: $\Theta(f(x)) = \{g(x) : \exists c_1, c_2, n_0, 0 \leq c_1\ f(x) \leq g(x) \leq c_2\ f(x), \forall x \geq x_0\}$.

power of m-th PU raises faster (in mutual interference environment or with superposition coding strategy).

- **(F5): Bound Conditions – Asymptotic Performance of Multiple Links.**
  CSH is a suitable approach to further increase both the capacity per link and the number of links per CSH group by sharing spectrum with unlicensed user. However, this increase is limited by CSHI and can never exceeds the performance of a CSHI-exempt model. Based on this concept, we could define simple upper bound conditions for the performance of CSH spectrum access as: 1) item using maximal transmit power ($P \to \infty$); and 2) item assuming CSHI-exempt. Although the two conditions are rather ideal and may not valid for a specific CSH model/group, they are essential in determining the performance bounds.

However, (F2-F5) jointly lead to an infinite SINR case ($\gamma_I \to \infty$), which is hard to clearly distinguish the performance of different CSH schemes. To characterize and improve the general and asymptotic spectrum access performance of CSH, proper performance metrics are needed. Moreover, the performance metric should be able to reflect the time efficiency loss in (F1).

B. Existing Performance Metrics

Data rate and error/outage probability are the most common performance metrics to determine the relative benefits of a CSH model [29]. Although these metrics are important, they do not tell the whole story of the CSH spectrum access performance. Recalling the main problems and features of CSH, one should determine the performance bounds, which may typically consider the conditions in (F5). Although the extreme case in (F5) may not exist in practice, they can be used as benchmark scenarios of how much a CSH model can improve its performance to the maximal extent by optimizing their protocol design and interference mitigation. Whereas, in terms of data rate/spectrum efficiency and error/outage probability metrics, fundamental bottlenecks emerge in these cases, and we have the following observations.

- The upper bounds of data rate and spectrum efficiency for different schemes are infinity, which can be explained as: $R \propto \log_2(1+\gamma_I)$ is monotonically increasing with respect to γ_I with conditions in (F2).
- The lower bounds of error/outage probabilities for different schemes are zero ($P_E/P_R \to 0$).

Thus, we find an interesting problem: the best performance (i.e. the bounds), these bounds may not distinguish among different CSH models. Therefore, the relative gaps of CSH techniques can not be obtained.

Unlike these metrics, multiplexing and diversity gains [30] can be distinct when $\gamma_I \to \infty$ in CSHI-exempt scheme, but they are inadequate to describe spectrum access ability considering (F5). At high SINR regime, multiplexing and diversity gains characterize the performance of a pair of users well. However, if a CSH system needs to justify its performance considering multiple links, phases to finish a cooperative transmission and the sum of transmitted symbols, better metrics should be proposed to exhibit the sum spectrum access ability and to exhibit distinct values for different CSH system model at high transmit SINR/power.

CSH encourages more concurrent co-channel access, less outage due to intra/inter-cell interference and better support for dual-hop cooperation, which motivates us to survey related metrics in [31]–[33]. Transport capacity is devised as the sum over each link of the product of the throughput per link times the distance between source and destination [31], typically resulting in an asymptotic scaling law as $O(\sqrt{\lambda})$, where λ is the density of transmitting nodes. However, their physical model focuses on a deterministic SINR model and thereby precludes the occurrence of outage [31], [34], which is not suitable for evaluating the upper bound of CSH spectrum access performance. Transmission capacity $c^\epsilon = \lambda^\epsilon b(1-\epsilon)$ [32] characterizes the density λ^ϵ of successful transmissions of a fixed spectral efficiency b and is subjected to a fixed outage probability constraint $\epsilon \in (0,1)$, but it is normally evaluated by considering a snapshot of a single-hop network. Moreover, considering (F3), λ is also fixed in a CSH group, and thus c^ϵ in this CSH scenario is more like a predetermined value than a performance metric. Random access transport capacity $C^{sh} = p_s\lambda_n \log_2(1+\gamma_I)R$ [33] captures the effect of outage and transmission range on the end-to-end throughput performance, where p_s, λ_n and R denote success probability, density of interfering nodes and point-to-point distance respectively. Nevertheless, performance bound of C^{sh} approaches infinity considering (F2) and (F5), and how to characterize multiple concurrent access considering (F5) is still undefined.

In CSH scenarios, we are more interested in the maximal concurrent access ability of network considering relaying, outage and numbers of co-existing devices. Although existing metrics accurately and instructively characterize most of the wireless scenarios, they are insufficient concerning the evaluation and design of CSH system models and schemes.

C. Key Ideas

Based on special features in (F1-F5) and existing metrics, the supplementary performance metrics for CSH must be able to

1) distinguish spectrum access ability of different CSH models at high transmit power, and find the specific bounds of spectrum access performance of a specific CSH system model,
2) reflect the time efficiency loss, the outage caused by CSHI and number of user pairs a CSH group can support,

In response to all the above questions, the contributions of this paper are as follows.

- For CSH systems, spectrum access level (SAL) is defined to capture the effect of CSHI and time efficiency loss, and can reflect the "capacity" of accessed links, which also has different upper bounds. SAL is close in meaning to the amount of maximal average exchanged data per cooperative phase, threading all the successful links. In addition, we define the user participation level (UPL) proportional to SAL per user.

- Upper bounds for SAL and UPL are derived for several CSH schemes. These upper bounds can also be determined directly from CSH models and protocols and may help to tentatively and preliminarily judge the highest performance of a specific CSH model.
- We propose a novel CSH system model that achieves the highest SALs compared to existing CSH models. To achieve the upper bound of SAL for proposed model, we design a novel CSHI mitigation strategy by exploiting source conferencing [35], [36] and signal space diversity [37] techniques.

This paper is organized as follows. Section II introduces the SAL and UPL metrics, where the upper bounds of SAL and UPL for existing CSH schemes are also summarized. The CSH system model and CSHI-exempt scheme are presented in Section III, and the performance evaluations are given in Section IV. We provide the numerical results to verify the proposed metrics and CSH system models with CSHI-exempt scheme in Section V. Section VI concludes the paper.

Notations: $\mathrm{E}\{x\}$, $\Re\{x\}$ and $\Im\{x\}$ denote the statistical expectation, real part and imaginary part of x. $|\mathcal{X}|$ denotes $Card(\mathcal{X})$ for set $\mathcal{X}$. Variables with bar (e.g. $\overline{\mathcal{X}}$) are upper bounds for origin variables (e.g. $\mathcal{X}$).

II. Spectrum Access Level and User Participation Level Metrics

Consider a CSH group $\mathcal{N}_{\text{CSH}}$ with primary nodes $\mathcal{N}_{\text{PU}}$ and secondary nodes $\mathcal{N}_{\text{SU}} = \mathcal{N}_{\text{SU,r}} \cup \mathcal{N}_{\text{SU,t}}$. Successful transmissions take place at rate R_{th} bit/s/Hz. Optimal power control is beyond the scope of this paper, because we intend to get general conclusions of the spectrum access ability for different CSH approaches. Perfect CSHI mitigation strategy, if exist, can be used to possibly obtain SINR $\gamma_I \to \infty$ when transmit power level $P \to \infty$ and (F2) is considered. We use $P \to \infty$ instead of $\gamma_I \to \infty$, because it is much easier for a scheme to ensure high transmit power level than directly to improve SINR. According to (F3), nodes in $\mathcal{N}_{\text{CSH}}$ have wireless communication interfaces working on the same band [38].

In the k-th phase, primary/secondary links $link \in \mathcal{E}_*^{(k)} \subseteq \mathcal{N}_* \times \mathcal{N}_*$ ($* \in \{\text{PU, SU}\}$) can be defined, where $\mathcal{E}_*^{(k)}$ is the set of active links in the k-th phase. Then, we denote $\mathcal{E}_{*,s}^{(k)} \subseteq \mathcal{E}_*^{(k)}$ as links with successful transmission (e.g. not in outage), and denote $\mathcal{E}_*$ as the set of all active links during cooperative phases T_c. Note that in multi-hop cases, $\mathcal{E}_*^{(k)}$ contains only the active hop of the primary/secondary multi-hop links in phase k. Since transmissions are on the same frequency, only time resource is considered, i.e., $\mathcal{FT} = T_c$. $T_c = \{1, ..., |T_c|\}$ is the set of phases for user cooperation and SUs' reward.[4] When an arbitrary transmitting node sends independent data to its receiver, $link$ is established with an error/outage probability $\mathcal{P}_{\mathcal{R}_{link}^{(k)}}(\gamma_{link})$ caused by CSHI, as well as occupying phase $k \in T_c$. Notice that there is directionality in $link$, i.e., $link$s of $\text{PU}_1 \to \text{PU}_2$ and $\text{PU}_2 \to \text{PU}_1$ are different. γ_{link} is the SINR of $link \in \mathcal{E}_*^{(k)}$. $K_{link}^{(k)}$ is the average sum of transmitted symbols of $link \in \mathcal{E}_*^{(k)}$ during the k-th phase. Assume that the transmit powers of PU and SU satisfy $P_P = P$ and $P_S = \eta P$, where P is the power level in (F4) to guarantee the transmit power of SU increasing in step with PU.

[4]For example, at least two phases are needed to finish a cooperative transmission by employing SUs as a half-duplex relays and an additional phase can be awarded to SUs for their own transmission ($|T_c| = 3$).

A. Definition of Spectrum Access Level

For evaluating the spectrum access ability for all PUs or SUs, it is useful to remind transport capacity, transmission capacity and random access capacity (see Section I-B). Likewise, in a CSH group $\mathcal{N}_{\text{CSH}}$ with users $* \in \{\text{PU, SU}\}$, the average maximal quantity of symbols pumped over successful end-to-end transmissions for all phases T_c can be measured as

$$\mathcal{S}_* = \sum_{k \in T_c} \sum_{link \in \mathcal{E}_*^{(k)}} \lim_{P \to \infty} K_{link}^{(k)} \left[1 - \mathcal{P}_{\mathcal{R}_{link}^{(k)}}(\gamma_{link}^{(k)})\right]. \quad (1)$$

Definition 1 (Spectrum Access Level): While evaluating the SAL, we limit each transmitter to send one symbol per phase. The SAL $\mathcal{A}_*$ can be defined as the average maximal sum rate (symbol/phase) for all successful end-to-end transmissions in $\mathcal{E}_*$:

$$\mathcal{A}_* = \frac{\mathcal{S}_*}{|T_c|}, \quad * \in \{PU,\ SU\}. \quad (2)$$

SAL shows the best spectrum access ability of a CSH model for any CSH scheme.[5] Then, $\mathcal{A}_*$ can be simply viewed as the average number of successful links per phase, indicating the time efficiency loss factor τ_*.

Theorem 1 (Physical Interpretation for SAL): If 1) the number of hops in each $link$ is $\mathcal{D}_*$, 2) each $link$ transmits statistically $K_{link}^{(k)} = \frac{1}{\mathcal{D}_*}$ symbols[6] with the end-to-end successful probability $\mathcal{P}_{S_{link}}$ in phase $k \in T_c$ and 3) the per phase average number of successful end-to-end transmissions/links is $E\{|\mathcal{E}_{*,s}|\}$, SAL is the number of average successful links times time efficiency.

$$\mathcal{A}_* = E\{|\mathcal{E}_{*,s}|\} \times \tau_*, \quad (3)$$

where $\tau_* = \mathcal{D}_* \times \mathcal{P}_*$ is time efficiency loss factor defined in (F1).

Proof: Based on (1), (2) and (F1), it is easy to obtain

$$\begin{aligned} A_* &= \frac{1}{|\,T_C\,|} \sum_{k \in T_C} \sum_{link \in \mathcal{E}_*^{(k)}} \lim_{P \to \infty} K_{link}^{(k)} \left[1 - \mathcal{P}_{\mathcal{R}_{link}^{(k)}}(\gamma_{link}^{(k)})\right] \\ &= \frac{|\,T_*\,|}{|\,T_C\,|} \frac{1}{\mathcal{D}_*} \times \left(E\{|\mathcal{E}_*^{(k)}|\} \mathcal{P}_{S_{link}}\right) \\ &= \tau_* \times E\{|\mathcal{E}_{*,s}|\}. \end{aligned}$$

□

Moreover, if a CSHI-exempt scheme can be found for a CSH model, we have

$$\lim_{P \to \infty} \mathcal{P}_{\mathcal{R}_{link}^{(k)}}(\gamma_{link}^{(k)}) = \mathcal{P}_{\mathcal{R}_{link}^{(k)}}(\infty) = 0. \quad (4)$$

[5]We refer to a CSH model as network topology and protocols, and a CSH scheme as cooperation behavior, coding and CSH mitigation strategies.

[6]This is possible if we consider a $\mathcal{D}_*$ hop link S-$\text{R}_1 \cdots \text{R}_{\mathcal{D}_*-1}$-D and a one hop link S-D, and each of them starts next transmission upon receiving the acknowledge receipt of previous packet. Thus, the average transmit rate for each hop is $\frac{1}{\mathcal{D}_*}$.

TABLE II
SPECTRUM ACCESS LEVEL

SAL ($*\in\{$PU, SU$\}$)	Implications for these metrics
$a_*(P)$	SAL with specific power level P, for a specific CSH scheme.
$\mathcal{A}_*$	Maximum SAL with maximal power, for a specific CSH scheme.
$\overline{\mathcal{A}}_*$	Maximum SAL with maximal power, if CSHI-free scheme exists.

Generally, assuming perfect interference mitigation approach exists, i.e., error/outage probabilities satisfying $P_{\mathcal{R}_{link}}=0$, the upper bound for a specific CSH model can be achieved by

$$\overline{\mathcal{A}}_* = \mathcal{A}_*\Big|_{P_{\mathcal{R}_{link}}=0} = \frac{\mathcal{S}_*}{|T_c|}\Big|_{P_{\mathcal{R}_{link}}=0}, * \in \{\text{PU, SU}\} \quad (5)$$

Definition 2 (SAL With Any Power Level): Based on Definition 1, the SINR of SAL may vary with transmit power level P. Then, we have

$$a_*(P) = \frac{1}{|T_c|}\sum_{k\in T_c}\sum_{link\in\mathcal{E}_*} K_{link}^{(k)}\left[1-\mathcal{P}_{\mathcal{R}_{link}^{(k)}}(\gamma_{link}^{(k)}(P))\right]. \quad (6)$$

Definition 3 (Achievable Upper Bound of SAL): For a given CSH model, the upper bound of SAL is achievable if there exists a perfect CSHI mitigation scheme with final end-to-end SINR γ_{link} satisfying $\lim_{P\to\infty}\gamma_{link}(P)=\infty$ for $\forall link\in\mathcal{E}_*$, where $*\in\{PU, SU\}$ and P is the transmit power level.

Definition 4 (Approaching the Upper Bound of SAL): For a given CSH model with specific scheme, the SAL can approach the upper bound with relative gap $\delta = 10\log_{10}\{(\overline{\mathcal{A}}_*-\mathcal{A}_*)/\overline{\mathcal{A}}_*\}$ dB, if the final end-to-end SINR (γ_{link}) of this scheme satisfies: $\lim_{P\to\infty}\gamma_{link}(P)$ is a constant, where $link\in\mathcal{E}_*$, $*\in\{PU, SU\}$ and P is the transmit power level. Note that the gap represents how efficiently the CSHI is mitigated, which can be a benchmark of CSH scheme design.

Remark 1: The mathematical relation between $a_*(P)$, A_* and $\overline{\mathcal{A}}_*$ can be given as follows

$$A_* = \lim_{P\to\infty} a_*(P), \quad \textit{for Condition-I}, \quad (7)$$

$$\overline{\mathcal{A}}_* = \mathcal{A}_*\Big|_{P_{\mathcal{R}_{link}}=0}, \quad \textit{for Condition-II}, \quad (8)$$

where Condition-I is "assuming power approaches infinity", and Condition II is "perfect CSHI mitigation scheme exists and is applied to the CSH model".

We also present Table II to conceptually distinguish these proposed SAL metrics.

B. User Capacity and Participation Level for Cooperative Spectrum Harvesting

Multiple PU and SU pairs can coexist in a CSH system, which reflects a "capacity" for supporting a number of user equipments reusing the same time-frequency resources. We define the user capacity for CSH system as the equivalent user number enrolled in CSH strategy: $N_*=2N_{*,pair}$, where $N_{*,pair}$ is number of end-to-end links.[7]

The utilization of time-frequency resources per user can reveal the spectrum access ability of each user, which also plays an important part in the evaluation for a CSH model. Then, based on user capacity and SAL, UPL can be defined as

$$\mathcal{L}_* = \frac{2\mathcal{S}_*}{|T_c|N_*} = \frac{2\mathcal{A}_*}{N_*} \text{ and } \overline{\mathcal{L}}_* = \frac{2\overline{\mathcal{A}}_*}{N_*} \; * \in \{\text{PU, SU}\}. \quad (9)$$

Similar to the Definition 2, we define UPL with any transmit power level as follows

$$l_*(P) = \frac{2}{N_*|T_c|}\sum_{k\in\mathcal{T}}\sum_{link\in\mathcal{E}_*} K_{link}^{(k)}\left[1-\mathcal{P}_{\mathcal{R}_{link}^{(k)}}(\gamma_{link}^{(k)}(P))\right], \quad (10)$$

where $*\in\{$PU, SU$\}$. If CSHI exists, following Definition 4, the gap between UPL $\mathcal{L}_*$ and its upper bound $\overline{\mathcal{L}}_*$ can be similarly defined as

$$\delta = 10\log_{10}(1-\mathcal{L}_*/\overline{\mathcal{L}}_*) \text{ dB}. \quad (11)$$

C. Discussions Based on CSHI Level

According to the definition of SAL, the "shortest board of the barrel" is outage/error probability $\mathcal{P}_{\mathcal{R}_{link}^{(k)}}(\gamma_{link}^{(k)}(P))$, of which the limit is highly dependent on the residual CSHI level in SINR. Based on the level of CSHI, we can classify CSH schemes into three classes.

1) CSHI-exempt. If a scheme is well-designed with efficient CSHI mitigation strategy, the scheme can achieve the upper bounds of SAL and UPL of the model. This is because $\mathcal{P}_{\mathcal{R}_{link}^{(k)}}(\gamma_{link}^{(k)}(P))$ will be zero if $P\to 0$.
2) Less CSHI. If a scheme encounters indelible CSHI, its rate or SINR will encounter a floor which indicates the highest achievable value. If the CSHI is small and the rate floor is much higher than R_{th}, the error/outage probability will remain in a level low enough to be neglected. Then, the scheme can approach but not achieve their upper bounds of SAL and UPL of the CSH model.
3) Severe CSHI. If a scheme encounters severe CSHI, its rate or SINR will encounter a floor which indicates the highest achievable value. If the rate floor is much lower than R_{th}, the error/outage probability will remain in non-negligible high level. Then, the SAL and UPL of this scheme are far below their upper bounds of CSH model.

[7]For unicast, $N_{*,pair}=\frac{1}{2}|\mathcal{N}_*|$; for multicast, $N_{*,pair}$ is the number of transmitters because all recievers have similar behavior and can be viewed as one user.

TABLE III
BASIC PARAMETERS FOR SCHEMES

System model	$\lvert T_c\rvert$	$\overline{\mathcal{S}}_{\text{PU}}$	$\overline{\mathcal{S}}_{\text{SU}}$	N_{PU}	N_{SU}
1	3	1	1	2	2
2	2	1	1	2	2
3	2	2	2	2	2
4	$L+1$	L	L	2	4
Proposed	2	4	2	4	2

TABLE IV
SAL AND UPL UPPER BOUNDS

System model	$\overline{\mathcal{A}}_{\text{PU}}$	$\overline{\mathcal{A}}_{\text{SU}}$	$\overline{\mathcal{L}}_{\text{PU}}$	$\overline{\mathcal{L}}_{\text{SU}}$
1	1/3	1/3	1/3	1/3
2	1/2	1/2	1/2	1/2
3	1	1	1	1
4	$\frac{L}{L+1}$	$\frac{L}{L+1}$	$\frac{L}{L+1}$	$\frac{L}{2(L+1)}$
Proposed	2	1	1	1

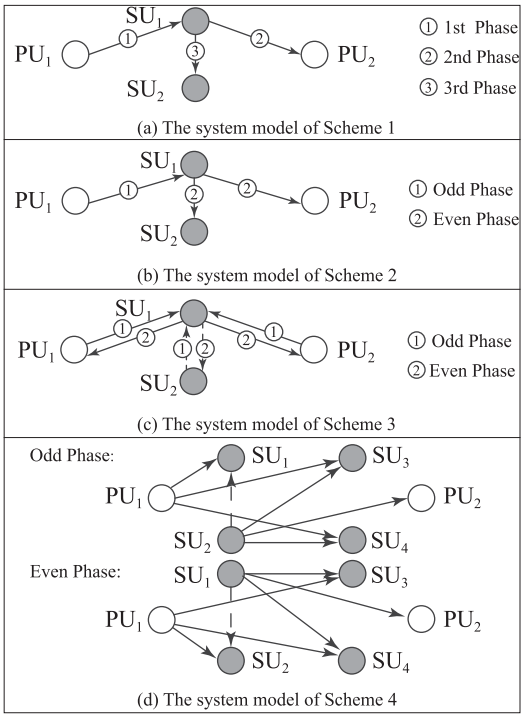

Fig. 1. The basic system models of existing cooperative spectrum harvesting schemes.

D. The Upper Bound of SAL/UPL for Existing CSH Models

If the CSH model and scheme are given, it is easy and straightforward (see Remark 2) to determine the upper bounds of the proposed SAL and UPL metrics using (F5), Definition 3 and Theorem 1. The results of evaluation are given in Table III and Table IV.

Here we review several CSH transmission models [17]–[19], [26], which are shown in Fig. 1. For a fair comparison, the direct-link between source and destination and multi-antenna setting are neglected, and we represent user group as a single user if user group exist[8] We refer to user group as all the users have the same behavior within one phase, such as multiple relays or users sharing a phase using TDMA, FDMA or CDMA.. Each user is equipped with omnidirectional antenna with regard to half-duplex mode. All transmissions within this network are assumed to be synchronized [17].

System model 1 can be found in [26], where SUs' transmitters act as cooperative relays for the PU in the first and second phases, and transmit their own data in the third phase. In the first phase of system model 2 [19], the D2D transmitter receives and decodes the signal broadcast by the cellular transmitter, and then regenerates the cellular signal and superposes it with the D2D signal. In the second phase, D2D transmitter broadcasts the composite signal to the cellular receiver and the D2D receiver. In the first phase of system model 3 [18], a chosen SU receives the signal from both PUs and the other SU simultaneously. In the second phase, the chosen SU uses a fraction of its transmit power to forward the PU signal, and uses the remaining power to transmit its own signal to the other SU. System model 4 is illustrated in [17], where two pairs of SUs get access to the spectrum occupied by a pair of PUs. Two of the four SUs act as two-path successive relays [39] and forward alternatively in even and odd phases. The transmitting SU uses a fraction of its transmit power to forward the primary signal, and uses the remaining power to transmit its own signal to the intended secondary receiver.

Remark 2 (Evaluating the Upper Bounds From CSH Model): With the assumptions from Definition 1 Theorem 1 and Remark 1, the upper bounds of SAL and UPL can be immediately evaluated by the CSH protocol and system model.

- ***Step 1: Establish Table III*** *- From CSH model, it is intuitive to determine $\lvert T_c\rvert$ and N_*. $\overline{\mathcal{S}}_*$ can be directly obtained by identifying the amount of symbols received by transceiver during T_c. For example, in Fig. 1(a), three phases are occupied and two PUs and one SUs are enrolled to finish one CSH transmission (which yields $\lvert T_c\rvert = 3$ and $N_{PU} = N_{SU} = 2$). During T_c, only one symbol can be received by primary and secondary receivers respectively (which yields $\overline{\mathcal{S}}_{PU} = \overline{\mathcal{S}}_{SU} = 1$).*
- ***Step 2: Calculate $\overline{\mathcal{A}}_*$ and $\overline{\mathcal{L}}_*$*** *- Based on (5) and (9), we can obtain $\overline{\mathcal{A}}_*$ and $\overline{\mathcal{L}}_*$.*

Remark 3: The SAL metric reveals how efficiently the spectrum is utilized by all considered users, while UPL metric reflects the spectrum access ability of an individual PU.

Remark 4: From the results of Table III and Table IV, we present some useful conclusions.

- *UPL shows how "actively" the user participates in spectrum utilization. If system parameters are chosen as in Theorem 1, the upper bound of UPL indicates average transmitted bits per user per unit time, i.e., UPL also reveals the multiplexing gain to a certain extent. Correspondingly, SAL means spectrum access efficiency.*

[8]Some of the models are not designed for direct link scenarios, which may increase SAL and UPL due to this additional link. We have to keep all the system models under similar assumption for a fair comparison.

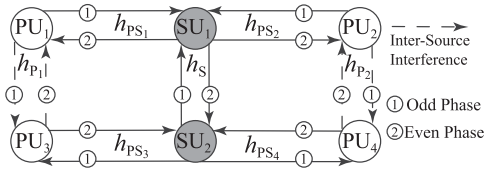

Fig. 2. The proposed system model.

- *Assuming perfect CSHI mitigation, higher SAL corresponds to larger number of supported communication pairs per phase. Whereas, high SAL may not result in high UPL, because UPL is guaranteed by every user sufficiently exchanging information.*

III. Proposed System Model and the CSHI-Exempt Scheme

To achieve higher SAL compared to conventional CSH models, the most intuitionistic method is to support as many user pairs as possible on the same band. Such approach provides very high SAL but suffer more CSHI. To exploit the full performance of this CSH model, we need to design a paradigm, i.e., a scheme well managing negative repercussions caused by CSHI.

A. Proposed CSH Model and Hypotheses for CSHI-Exempt Scheme

We consider one active secondary pair (SU_1-SU_2) tries to share the time-frequency resource of two primary pairs (PU_1-PU_2 and PU_3-PU_4) via alternatively relaying. The channel coefficients are assumed remaining static during each frame [37] and the complex channel coefficients of links PU_1-SU_1, PU_2-SU_1, PU_3-SU_2, PU_4-SU_2, PU_1-PU_3, PU_2-PU_4 and SU_1-SU_2 are denoted by h_{PS_1},h_{PS_2}, h_{PS_3}, h_{PS_4}, h_{P_1}, h_{P_2} and h_{S} respectively. Following [21] and [40], we assume reciprocal channel, i.e., $h_{ij} = h_{ji}$ for nodes i and j. $|h_k|$ and $\angle k$ denote the amplitude and the phase of channel coefficient h_k ($k \in \{\mathrm{PS}_1, \mathrm{PS}_2, \mathrm{PS}_3, \mathrm{PS}_4, \mathrm{P}_1, \mathrm{P}_2, \mathrm{S}\}$) respectively. The background noise is assumed to be independent additive white Gaussian noise (AWGN) with variance σ_n^2. $s_{\mathrm{PU}_p}^{(k)}$ and $s_{\mathrm{SU}_q}^{(k)}$ denotes the original symbols for BS, PU_p and SU_q at the k-th phase ($p \in \{1,2,3,4\}$ and $q \in \{1,2\}$), respectively. We consider omni-directional half-duplex radio nodes only.

The proposed CSH model is shown in Fig. 2 and we follow assumptions B1-B3 to facilitate the CSHI mitigation and the performance evaluation.

B1: Consider the scenario that the direct link between the primary communication pair PU_1-PU_2 (PU_3-PU_4) does not exist, which motivates PUs to employ SUs as relay nodes to help to exchanging data. Thus, PU_1&PU_3 side is unable to interfere PU_2&PU_4 side, and vice versa. Assuming PU_1-PU_3 and PU_2-PU_4 are also connected by out-of-band source conferencing links respectively,[9] PUs in these pairs can exchange the information of inter-source interferences (in Fig. 2).

B2: Each user has the local channel state information (CSI). PUs can acquire the CSI (h_{S}) between SUs and the amplifying factor of SU. This can be explained by the fact that SUs intended to share PUs' spectrum cooperatively and they are willing to sharing their local CSI and amplifying factors.

B3: According to Theorem 1, for the convenience of evaluation, one transmitter sends one bit in a symbol to its intended receiver within one phase.

In Fig. 2, CSHI arises since the three senders share the same spectrum non-orthogonally. Note that *intrinsic orthogonality* exists between the in-phase and the quadrature component of a complex constellation. Based on this nature, Sun *et al*. [37] exploited the signal space diversity (SSD) to separate two non-orthogonal links, which motives us to design the techniques to mitigate CSHI. To demodulate the signals only based on the real or the imaginary component, signal constellation must be rotated [37]. Specifically, if u is the original complex constellation taking values from an M-ary alphabet χ, the transmitted symbol will be $x = ue^{j\phi}$, where ϕ is chosen in such a way that no two symbols have the same coordinate. That is, for any $p \neq q$,

$$\Re\{x^p\} \neq \Re\{x^q\}, \quad \Im\{x^p\} \neq \Im\{x^q\}, \ \forall x^p, \ x^q \in e^{j\phi}\chi. \quad (12)$$

Prior to the transmission in the proposed CSH scheme, constellation rotation is applied to every symbol with the angle ϕ chosen from [37]. Each transmit symbol $s_*^{(k)}$ is constellation rotated before precoding, and the symbol power satisfies $\mathbb{E}\{|\Re\{s_*^{(k)}\}|^2\} = 1$ ($* \in \{\mathrm{PU}_m, \mathrm{SU}_n\}, m \in \{1,2,3,4\}$, $n \in \{1,2\}$).

B. Signal Transmission Model

At the k-th phase (k is odd) the transmit symbols from active transmitters are precoded as

$$x_{\mathrm{PU}_1}^{(k)} = j\sqrt{P_P}\, s_{\mathrm{PU}_1}^{(k)} e^{-\angle_{\mathrm{PS}_1}}, \quad (13)$$

$$x_{\mathrm{PU}_2}^{(k)} = j\sqrt{P_P}\, s_{\mathrm{PU}_2}^{(k)} e^{-\angle_{\mathrm{PS}_2}}, \quad (14)$$

$$x_{\mathrm{SU}_2}^{(k)} = \sqrt{\frac{P_S}{2}}\left[\alpha_{\mathrm{SU}_2} y_{\mathrm{SU}_2}^{(k-1)} + s_{\mathrm{SU}_2}^{(k)}\right] e^{-\angle_{\mathrm{S}}}, \quad (15)$$

where the $\alpha_{\mathrm{SU}_2} = \sqrt{\frac{1}{\mathrm{E}\{|y_{\mathrm{SU}_2}|^2\}}}$. At the k-th phase, the signals received by PU_3, PU_4 and SU_1 are

$$y_{\mathrm{PU}_3}^{(k)} = h_{\mathrm{P}_1} x_{\mathrm{PU}_1}^{(k)} + h_{\mathrm{PS}_3} x_{\mathrm{SU}_2}^{(k)} + n_{\mathrm{PU}_3}^{(k)}, \quad (16)$$

$$y_{\mathrm{PU}_4}^{(k)} = h_{\mathrm{P}_2} x_{\mathrm{PU}_2}^{(k)} + h_{\mathrm{PS}_4} x_{\mathrm{SU}_2}^{(k)} + n_{\mathrm{PU}_4}^{(k)}, \quad (17)$$

$$y_{\mathrm{SU}_1}^{(k)} = h_{\mathrm{PS}_1} x_{\mathrm{PU}_1}^{(k)} + h_{\mathrm{PS}_2} x_{\mathrm{PU}_2}^{(k)} + h_{\mathrm{S}} x_{\mathrm{SU}_2}^{(k)} + n_{\mathrm{SU}_1}^{(k)}. \quad (18)$$

At the $(k+1)$-th phase the transmit symbols are precoded as follows

$$x_{\mathrm{PU}_3}^{(k+1)} = j\sqrt{P_P}\, s_{\mathrm{PU}_3}^{(k+1)} e^{-\angle_{\mathrm{PS}_3}} \quad (19)$$

$$x_{\mathrm{PU}_4}^{(k+1)} = j\sqrt{P_P}\, s_{\mathrm{PU}_4}^{(k+1)} e^{-\angle_{\mathrm{PS}_4}} \quad (20)$$

$$x_{\mathrm{SU}_1}^{(k+1)} = \sqrt{\frac{P_S}{2}}\left[\alpha_{\mathrm{SU}_1} y_{\mathrm{SU}_1}^{(k)} + s_{\mathrm{SU}_1}^{(k+1)}\right] e^{-\angle_{\mathrm{S}}}, \quad (21)$$

[9]This corresponds to the presence of backhaul between two primary base stations, or D2D links between two mobile primary users, or with the help of an out-of-band relay deployed at the common cell boundary [35], [36]. The assumption for source conferencing may not valid in practice, bu we employ it to uncover a CSHI-exempt scheme for interpretation of achieving SAL/UPL upper bounds.

where $\alpha_{\mathrm{SU}_1}=\sqrt{\frac{1}{\mathrm{E}\{|y_{\mathrm{SU}_1}|^2\}}}$. The signals received by PU_1, PU_2 and SU_2 are

$$y_{\mathrm{PU}_1}^{(k+1)}=h_{\mathrm{P}_1}x_{\mathrm{PU}_3}^{(k+1)}+h_{\mathrm{PS}_1}x_{\mathrm{SU}_1}^{(k+1)}+n_{\mathrm{PU}_1}^{(k+1)}, \tag{22}$$

$$y_{\mathrm{PU}_2}^{(k+1)}=h_{\mathrm{P}_2}x_{\mathrm{PU}_4}^{(k+1)}+h_{\mathrm{PS}_2}x_{\mathrm{SU}_1}^{(k+1)}+n_{\mathrm{PU}_2}^{(k+1)}, \tag{23}$$

$$y_{\mathrm{SU}_2}^{(k+1)}=h_{\mathrm{PS}_3}x_{\mathrm{PU}_3}^{(k+1)}+h_{\mathrm{PS}_4}x_{\mathrm{PU}_4}^{(k+1)}+h_{\mathrm{S}}x_{\mathrm{SU}_1}^{(k+1)}+n_{\mathrm{SU}_2}^{(k+1)}. \tag{24}$$

The CSHI can be observed existing in every phase, which prevents the SAL and UPL from achieving upper bounds. Thus, CSHI mitigation strategy is needed, and simple signal processing technique should be designed to extract intended symbols.

C. CSHI Mitigation and Signal Extraction Techniques

We focus on an arbitrary $(k+1)$-th phase to exhibit the CSHI mitigation for the observations of receivers PU_1, PU_2, and SU_2. Three intended symbols (primary symbol $s_{\mathrm{PU}_n}^{(k)}, n\in\{1,2\}$ relayed by SU and secondary symbol $s_{\mathrm{SU}_1}^{(k+1)}$) coexist with mutual interferences. After CSHI mitigation, simple formulas should be determined to extract intended data.

1) Primary System: The observation of PU_1 at the $(k+1)$-th phase is given in (22). Replace the $y_{\mathrm{SU}_1}^{(k)}$ in (21) by (18), and use the result to replace $x_{\mathrm{SU}_1}^{(k+1)}$ in (22). Then, we have the identical transformation for (22) as

$$y_{\mathrm{PU}_1}^{(k+1)}=\alpha_{\mathrm{SU}_1}h_{\mathrm{PS}_1}\sqrt{\frac{P_S}{2}}e^{-\angle_{\mathrm{S}}}\Big\{\left(h_{\mathrm{PS}_1}x_{\mathrm{PU}_1}^{(k)}+h_{\mathrm{PS}_2}x_{\mathrm{PU}_2}^{(k)}\right)+h_{\mathrm{S}}x_{\mathrm{SU}_2}^{(k)}+s_{\mathrm{SU}_1}^{(k+1)}+n_{\mathrm{SU}_1}^{(k)}\Big\}+h_{\mathrm{P}_1}x_{\mathrm{PU}_3}^{(k+1)}+n_{\mathrm{PU}_1}^{(k+1)}. \tag{25}$$

Note that both (25) and (16) have the common variable $x_{\mathrm{SU}_2}^{(k)}$, and (16) may be modified to

$$x_{\mathrm{SU}_2}^{(k)}=\frac{1}{h_{\mathrm{PS}_3}}\left[y_{\mathrm{PU}_3}^{(k)}-h_{\mathrm{P}_1}x_{\mathrm{PU}_1}^{(k)}-n_{\mathrm{PU}_3}^{(k)}\right]. \tag{26}$$

Eq. (26) can be substituted together with (14) into (25), and then we obtain the identical formula of PU_1's observation with indications of different interferences and additive noise as follows

$$y_{\mathrm{PU}_1}^{(k+1)}=\alpha_{\mathrm{SU}_1}\sqrt{\frac{P_S}{2}}\left[j|h_{\mathrm{PS}_2}|\sqrt{P_P}s_{\mathrm{PU}_2}^{(k)}+s_{\mathrm{SU}_1}^{(k+1)}\right]h_{\mathrm{PS}_1}e^{-\angle_{\mathrm{S}}}+I_{\mathrm{PU}_1}^{(k+1)}+I_{\mathrm{PU}_3}^{(k+1)}+w_{\mathrm{PU}_1}^{(k+1)}, \tag{27}$$

where $I_{\mathrm{PU}_1}^{(k+1)}=\left(\frac{h_{\mathrm{PS}_1}}{e^{\angle_{\mathrm{S}}}}-\frac{|h_{\mathrm{S}}|h_{\mathrm{P}_1}}{h_{\mathrm{PS}_3}}\right)\alpha_{\mathrm{SU}_1}h_{\mathrm{PS}_1}\sqrt{\frac{P_S}{2}}x_{\mathrm{PU}_1}^{(k)}$, $I_{\mathrm{PU}_3}^{(k+1)}=\frac{\alpha_{\mathrm{SU}_1}h_{\mathrm{PS}_1}|h_{\mathrm{S}}|\sqrt{\frac{P_S}{2}}}{h_{\mathrm{PS}_3}}y_{\mathrm{PU}_3}^{(k)}+h_{\mathrm{P}_1}x_{\mathrm{PU}_3}^{(k+1)}$, and $w_{\mathrm{PU}_1}^{(k+1)}=-\frac{\alpha_{\mathrm{SU}_1}h_{\mathrm{PS}_1}|h_{\mathrm{S}}|\sqrt{\frac{P_S}{2}}}{h_{\mathrm{PS}_3}}n_{\mathrm{PU}_3}^{(k)}+\alpha_{\mathrm{SU}_1}h_{\mathrm{PS}_1}\sqrt{\frac{P_S}{2}}e^{-\angle_{\mathrm{S}}}n_{\mathrm{SU}_1}^{(k)}+n_{\mathrm{PU}_1}^{(k+1)}$.

The above signal processing separates each CSHI term. $I_{\mathrm{PU}_1}^{(k+1)}$ can be canceled as known interference and the inter-source interference $I_{\mathrm{PU}_3}^{(k+1)}$ can be canceled via source conferencing.

After CSHI cancellation, the signal in (27) is given by

$$Y_{\mathrm{PU}_1}^{(k+1)}=\alpha_{\mathrm{SU}_1}h_{\mathrm{PS}_1}\sqrt{\frac{P_S}{2}}\left[j|h_{\mathrm{PS}_2}|\sqrt{P_P}s_{\mathrm{PU}_2}^{(k)}+s_{\mathrm{SU}_1}^{(k+1)}\right]e^{-\angle_{\mathrm{S}}}+w_{\mathrm{PU}_1}^{(k+1)}. \tag{28}$$

Then, PU_1's intended symbol $s_{\mathrm{PU}_2}^{(k)}$ carried in (28) can be extracted by (29).

$$\begin{aligned}\tilde{s}_{\mathrm{PU}_2}^{(k)}&=\frac{1}{\alpha_{\mathrm{SU}_1}|h_{\mathrm{PS}_2}|\sqrt{\frac{P_S}{2}}}\Im\left\{\frac{Y_{\mathrm{PU}_1}^{(k+1)}e^{\angle_{\mathrm{S}}}}{h_{\mathrm{PS}_1}}\right\}\\&=\sqrt{P_P}s_{\mathrm{PU}_2}^{(k)}+\tilde{n}_{\mathrm{PU}_2}^{(k)},\end{aligned} \tag{29}$$

where $\tilde{n}_{\mathrm{PU}_2}^{(k)}\sim N\left(0,\left(1+\frac{|h_{\mathrm{S}}|^2}{|h_{\mathrm{PS}_3}|^2}+\frac{2}{\beta_{\mathrm{SU}_1}^2|h_{\mathrm{PS}_2}|^2}\right)\frac{\sigma_n^2}{2|h_{\mathrm{PS}_2}|^2}\right)$, $\beta_{\mathrm{SU}_1}=\sqrt{\frac{P_S}{P_P\left(|h_{\mathrm{PS}_1}|^2+|h_{\mathrm{PS}_2}|^2\right)+P_S|h_{\mathrm{S}}|^2+\sigma_n^2}}$ and

$$\tilde{n}_{\mathrm{PU}_2}^{(k)}=-\Im\left\{\frac{h_{\mathrm{S}}n_{\mathrm{PU}_3}^{(k)}}{|h_{\mathrm{PS}_2}|h_{\mathrm{PS}_3}}\right\}+\Im\left\{\frac{n_{\mathrm{SU}_1}^{(k)}}{|h_{\mathrm{PS}_2}|}\right\}+\frac{\sqrt{2}}{\beta_{\mathrm{SU}_1}|h_{\mathrm{PS}_2}|}\Im\left\{\frac{e^{\angle_{\mathrm{S}}}n_{\mathrm{PU}_1}^{(k+1)}}{h_{\mathrm{PS}_1}}\right\}. \tag{30}$$

Similarly, it is easy to extract $s_{\mathrm{PU}_1}^{(k)}$ by (31).

$$\begin{aligned}\tilde{s}_{\mathrm{PU}_1}^{(k)}&=\frac{1}{\alpha_{\mathrm{SU}_1}|h_{\mathrm{PS}_1}|\sqrt{\frac{P_S}{2}}}\Im\left\{\frac{Y_{\mathrm{PU}_2}^{(k+1)}e^{\angle_{\mathrm{S}}}}{h_{\mathrm{PS}_2}}\right\}\\&=\sqrt{P_P}s_{\mathrm{PU}_1}^{(k)}+\tilde{n}_{\mathrm{PU}_1}^{(k)},\end{aligned}$$

where $\tilde{n}_{\mathrm{PU}_1}^{(k)}\sim N\left(0,\left(1+\frac{|h_{\mathrm{S}}|^2}{|h_{\mathrm{PS}_4}|^2}+\frac{2}{\beta_{\mathrm{SU}_1}^2|h_{\mathrm{PS}_1}|^2}\right)\frac{\sigma_n^2}{2|h_{\mathrm{PS}_1}|^2}\right)$ and

$$\tilde{n}_{\mathrm{PU}_1}^{(k)}=-\Im\left\{\frac{h_{\mathrm{S}}n_{\mathrm{PU}_4}^{(k)}}{|h_{\mathrm{PS}_1}|h_{\mathrm{PS}_4}}\right\}+\Im\left\{\frac{n_{\mathrm{SU}_1}^{(k)}}{|h_{\mathrm{PS}_1}|}\right\}+\frac{\sqrt{2}}{\beta_{\mathrm{SU}_1}|h_{\mathrm{PS}_1}|}\Im\left\{\frac{e^{\angle_{\mathrm{S}}}n_{\mathrm{PU}_2}^{(k+1)}}{h_{\mathrm{PS}_2}}\right\}.$$

2) Secondary System: The observation of SU_2 at $(k+1)$-th phase is given by (24). Substitute (18) into (21) to replace $y_{\mathrm{SU}_1}^{(k)}$, and the result is used to replace $x_{\mathrm{SU}_1}^{(k+1)}$ in (24). Then we obtain

$$\begin{aligned}&y_{\mathrm{SU}_2}^{(k+1)}\\&=\alpha_{\mathrm{SU}_1}\sqrt{\frac{P_S}{2}}|h_{\mathrm{S}}|\left[h_{\mathrm{PS}_1}x_{\mathrm{PU}_1}^{(k)}+h_{\mathrm{PS}_2}x_{\mathrm{PU}_2}^{(k)}\right]+\sqrt{\frac{P_S}{2}}|h_{\mathrm{S}}|s_{\mathrm{SU}_1}^{(k+1)}\\&\quad+\left[h_{\mathrm{PS}_3}x_{\mathrm{PU}_3}^{(k+1)}+h_{\mathrm{PS}_4}x_{\mathrm{PU}_4}^{(k+1)}\right]+I_{\mathrm{SU}_2}^{(k+1)}+w_{\mathrm{SU}_2}^{(k+1)},\end{aligned} \tag{31}$$

where $w_{\mathrm{SU}_2}^{(k+1)}=\alpha_{\mathrm{SU}_1}\sqrt{\frac{P_S}{2}}|h_{\mathrm{S}}|n_{\mathrm{SU}_1}^{(k)}+n_{\mathrm{SU}_2}^{(k+1)}$ and $I_{\mathrm{SU}_2}^{(k+1)}=\alpha_{\mathrm{SU}_1}\sqrt{\frac{P_S}{2}}|h_{\mathrm{S}}|h_{\mathrm{S}}x_{\mathrm{SU}_2}^{(k)}$.

Replace $x_{\mathrm{PU}_1}^{(k)}$, $x_{\mathrm{PU}_2}^{(k)}$, $x_{\mathrm{PU}_3}^{(k)}$ and $x_{\mathrm{PU}_4}^{(k)}$ in (31) by (13), (14), (19) and (20) respectively. Then, we obtain the identical formula of SU_2's observation with clear indications of interference and noise terms:

$$y_{\mathrm{SU}_2}^{(k+1)}=\sqrt{\frac{P_S}{2}}|h_{\mathrm{S}}|s_{\mathrm{SU}_1}^{(k+1)}+I_{\mathrm{SU}_2}^{(k+1)}+jI_{\mathrm{PU}}^{(k+1)}+w_{\mathrm{SU}_2}^{(k+1)}, \tag{32}$$

where $I_{\text{PU}}^{(k+1)} = \alpha_{\text{SU}_1}\sqrt{\frac{P_S P_P}{2}}|h_{\text{S}}|\sum_{m=1}^{2}|h_{\text{PS}_m}|s_{\text{PU}_m}^{(k)} + \sqrt{P_P}\sum_{m=3}^{4}|h_{\text{PS}_m}|s_{\text{PU}_m}^{(k+1)}$. After canceling the known interference $I_{\text{SU}_2}^{(k+1)}$, the signal in (32) is given by

$$Y_{\text{SU}_2}^{(k+1)} = \sqrt{\frac{P_S}{2}}|h_{\text{S}}|s_{\text{SU}_1}^{(k+1)} + jI_{\text{PU}}^{(k+1)} + w_{\text{SU}_2}^{(k+1)}. \quad (33)$$

Note that $jI_{\text{PU}}^{(k+1)}$ is orthogonal to the intended signal $s_{\text{PU}_1}^{(k+1)}$. Then, the intended symbol $s_{\text{SU}_1}^{(k+1)}$ of SU_2 can be extracted from (34).

$$\tilde{s}_{\text{SU}_1}^{(k+1)} = \frac{\sqrt{2}}{|h_{\text{S}}|}\Re\left\{Y_{\text{SU}_2}^{(k+1)}\right\} = \sqrt{P_S}s_{\text{SU}_2}^{(k)} + \tilde{n}_{\text{SU}_1}^{(k+1)}, \quad (34)$$

where $\tilde{n}_{\text{SU}_1}^{(k+1)} = \Re\{\beta_{\text{SU}_1}n_{\text{SU}_1}^{(k)} + \frac{\sqrt{2}n_{\text{SU}_2}^{(k+1)}}{|h_{\text{S}}|}\}$ and $\tilde{n}_{\text{SU}_1}^{(k+1)} \sim N\left(0, \left(\beta_{\text{SU}_1}^2 + \frac{2}{|h_{\text{S}}|^2}\right)\frac{\sigma_n^2}{2}\right)$.

IV. Performance Evaluation for the Proposed CSH Model

The upper bounds of SAL and UPL for the proposed CSH model have been given in Table IV, which can be determined directly by the system model with the assumptions in Section II-D. However, according to Definition 3, the upper bounds are not achievable if the CSHI is not efficiently mitigated. Thus, in this section we should first ensure that the final end-to-end SINR γ_{link} of the proposed scheme satisfies $\lim_{P\to\infty}\gamma_{link}(P) = \infty$ for $\forall link \in \mathcal{E}_*$, $* =$ PU or SU, and then use the results to calculate the SAL and UPL for the proposed CSH model.

A. End-to-End SINR of the Proposed Scheme

1) PU at the $(k+1)$-th Phase: We take the link $\text{PU}_2 \to \text{PU}_1$ as an example to show that the PU's end-to-end SINR satisfies Definition 3. The limit of the end-to-end SINR with respect to link $\text{PU}_2 \to \text{PU}_1$ can be calculated from (29) and given by

$$\lim_{P\to\infty}\gamma_{\text{PU}_2\text{PU}_1}^{(k+1)} = \frac{2|h_{\text{PS}_1}|^2\lim\limits_{P\to\infty}P}{\left(1 + \frac{|h_{\text{S}}|^2}{|h_{\text{PS}_4}|^2} + \frac{2}{|h_{\text{PS}_1}|^2\lim\limits_{P\to\infty}\beta_{\text{SU}_1}^2}\right)\sigma_n^2} = \infty, \quad (35)$$

where $\lim\limits_{P\to\infty}\beta_{\text{SU}_1}^2 = \frac{\eta}{\left(|h_{\text{PS}_1}|^2+|h_{\text{PS}_2}|^2\right)+\eta|h_{\text{S}}|^2+\sigma_n^2}$ is finite.

Similarly, we can determine that $\lim\limits_{P\to\infty}\gamma_{\text{PU}_1\text{PU}_2}^{(k+1)} = \infty$.

2) SU at the k-th and $(k+1)$-th Phase: The limit of the end-to-end SINR with respect to link $\text{SU}_1 \to \text{SU}_2$ can be calculated from (34) and given by

$$\lim_{P\to\infty}\gamma_{\text{SU}_1\text{SU}_2}^{(k+1)} = \frac{\eta\lim\limits_{P\to\infty}P}{\left(\lim\limits_{P\to\infty}\beta_{\text{SU}_1}^2 + \frac{2}{|h_{\text{S}}|^2}\right)\frac{\sigma_n^2}{2}} = \infty. \quad (36)$$

Similarly, we have $\lim\limits_{P\to\infty}\gamma_{\text{SU}_2\text{SU}_1}^{(k)} = \infty$.

Remark 5: Eq. (35) and (36) show that after CSHI mitigation and signal extraction the end-to-end SINRs of PU and SU satisfie Definition 3. Thus, CSHI mitigation strategy ensures that the proposed CSH model achieves the upper bounds of SAL and UPL. Note that the CSHI mitigation is based on assumptions B1 and B2, which means the reachability of upper bounds of the metrics for the proposed CSH model is conditional.

B. Spectrum Access Level

1) SAL for the Primary System: Due to the repetitive feature of even and odd phases, we can focus on two successive phases, i.e., $T_c = \{k\text{-th phase}, (k+1)\text{-th phase}\}$ and $|T_c| = 2$. Based on the monotonous and continuous of $\mathcal{P}_{\mathcal{R}_{ab}^{(k)}}(\gamma_{ab}^{(k)})$ with respect to $\gamma_{ab}^{(k)}$, we can easily calculate the average number of delivered symbols pumped over successful links at $(k+1)$-th phase as

$$\begin{aligned}\mathcal{S}_{\text{PU}}^{(k+1)} &= \sum_{ab\in\mathcal{E}_{\text{PU}}} K_{ab}^{(k+1)}\left[1 - \mathcal{P}_{\mathcal{R}_{ab}^{(k+1)}}(\lim_{P\to\infty}\gamma_{ab}^{(k+1)})\right] \\ &= \sum_{ab\in\{\text{PU}_2\text{PU}_1,\text{PU}_1\text{PU}_2\}}[1 - Pr(\infty < R_{th})] \\ &= 2. \end{aligned} \quad (37)$$

Similarly, we can obtain $\mathcal{S}_{\text{PU}}^{(k)}$ as

$$\begin{aligned}\mathcal{S}_{\text{PU}}^{(k)} &= \sum_{ab\in\{\text{PU}_3\text{PU}_4,\text{PU}_4\text{PU}_3\}}\left[1 - \mathcal{P}_{\mathcal{R}_{ab}^{(k+1)}}(\gamma_{ab}^{(k+1)})\right]_{\gamma_{ab}^{(k+1)}=\infty} \\ &= 2. \end{aligned} \quad (38)$$

Therefore, the SAL for primary system can be obtained based on (2) as

$$\mathcal{A}_{\text{PU}} = \frac{\mathcal{S}_{\text{PU}}^{(k)} + \mathcal{S}_{\text{PU}}^{(k+1)}}{|T_c|} = 2. \quad (39)$$

2) SAL for the Secondary System: The average quantity of successfully delivered symbols for all successful secondary links and at $(k+1)$-th and k-th phases can be calculated as

$$\mathcal{S}_{\text{SU}}^{(k+1)} = \left[1 - \mathcal{P}_{\mathcal{R}_{ij}^{(k+1)}}(\gamma_{ij}^{(k+1)})\right]_{ij=\text{SU}_1\text{SU}_2,\ \gamma_{ij}^{(k+1)}=\infty} = 1, \quad (40)$$

$$\mathcal{S}_{\text{SU}}^{(k)} = \left[1 - \mathcal{P}_{\mathcal{R}_{ij}^{(k)}}(\gamma_{ij}^{(k)})\right]_{ij=\text{SU}_2\text{SU}_1,\ \gamma_{ij}^{(k+1)}=\infty} = 1. \quad (41)$$

Therefore, the SAL for secondary system can be obtained based on (2) as

$$\mathcal{A}_{\text{SU}} = \frac{\mathcal{S}_{\text{SU}}^{(k)} + \mathcal{S}_{\text{SU}}^{(k+1)}}{|T_c|} = 1. \quad (42)$$

C. User Capacity and Participation Level

It is straightforward to obtain the end-to-end user capacities from system model: $N_{\text{PU}} = 4$ and $N_{\text{SU}} = 2$. Based on SAL, the UPLs for primary and secondary system are obtained as

$$\mathcal{L}_{\text{PU}} = \frac{2\mathcal{A}_{\text{PU}}}{N_{\text{PU}}} = 1 \text{ and } \mathcal{L}_{\text{SU}} = \frac{2\mathcal{A}_{\text{SU}}}{N_{\text{SU}}} = 1. \quad (43)$$

Remark 6: From (39), (42) and (43), we can conclude that the proposed CSH model can achieve the upper bounds of SAL and UPL shown in Table IV.

V. Numerical Results

Numerical results are given here to verify the proposed metrics and the performance of proposed CSH model. For a fair comparison, the direct primary link is not considered in all cases. BPSK modulation is adopted and frame length is $L+1=33$. We set $P_S=P_P$ and the relaying SU splits its power equally for own data and PU's data in the comparing schemes with superposition coding. All channel coefficients are distributed with the Rayleigh fading model along with the path loss as $h_{ab}=r_{ab}\sqrt{d_{ab}^{-\lambda}}$, where r_{ab} is a zero-mean, unit-variance complex Gaussian variable, d_{ab} is the distance between nodes a and b (which are set to be 3 for PU$_p$-SU$_m$ link, 2 for PU$_q$-SU$_m$ link, and 2 for SU$_1$-SU_2 link ($p\in\{1,2\}$, $q\in\{3,4\}$ and $m\in\{1,2\}$), $\lambda=3$ is the path loss factor. The power of the AWGN term of each link is set equally to $\sigma^2=1$. The primary and secondary rate thresholds are assumed equal to $R_{th}=0.4$.[10] The legend "P" represents the power level P introduced in Section II. For comparison, we consider the conventional CSH models [17], [19], [20], [26] in introduction section, and each system model applies the CSH scheme proposed in the same article respectively. Notations "Scheme 1" to "Scheme 4" correspond to the CSH model shown in Fig. 1, and the notation "Proposed" corresponds to our proposed CSH model with the CSHI-exempt scheme. SAL and UPL are measured by the definitions proposed in this paper.

A. SALs and End-to-End Capacities of Primary Systems

Fig. 3(a) and Fig. 3(b) present the numerical results for the spectrum access level and end-to-end capacity of primary systems, respectively. In Section II-C, we classify CSH schemes into three classes based on the level of residual CSHI. Following the three classes, we detailedly present the observations and conclusions from the numerical results depicted in Fig. 3(a) and Fig. 3(b).

- CSHI-exempt: Scheme 1 and the proposed scheme.
  1) When the transmit power level (P) is relatively low, the SALs (a_{PU}) of these two schemes keep rising with the increasing P. At high power level, the two schemes achieve their maximal SALs as $\frac{1}{3}$ and 2 respectively, which are the upper bounds (in Table IV) concerning their system models.
  2) The observations of 1) can be explained by the facts in Fig. 3(b), which exhibit no floors in the end-to-end capacity curves of these two schemes. As the power level is high enough, the outage/error probability is $\mathcal{P}_{\mathcal{R}_{link}^{(k)}}\left(\gamma_{link}^{(k)}(P)\right)=0$ and SINR is $\gamma_{lilnk}(P)=\infty$, which satisfies Definition 3.
  3) It can be observed from Fig. 3(a) and 3(b) that the CSHI-exempt schemes can achieve the best distinguishable SALs of the two CSH models.

[10]In practice, the threshold depends on the type of service. For example, online FLASH video and picture viewing services may be supported well by low successful rate; And the real-time transmission of 4K or 8K video may result in high rate requirement. Here we assume $R_{th}=0.4$ for clearly displaying identifiable simulation results in a single figure.

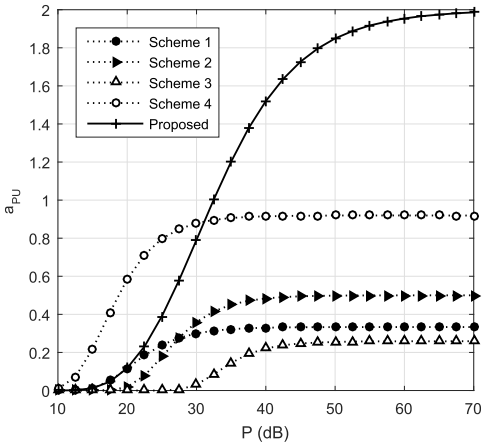

(a) a_{PU}

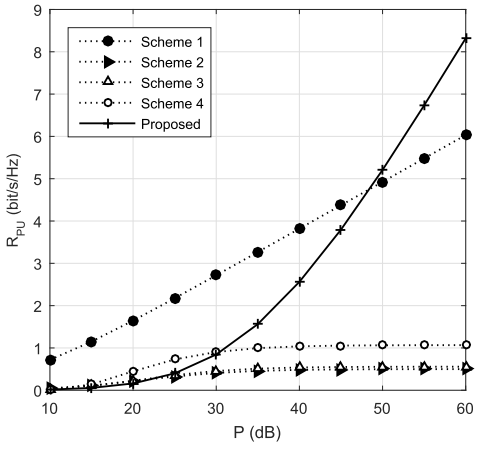

(b) R_{PU}

Fig. 3. Spectrum access level a_{PU} and end-to-end capacity R_{PU} of primary system at different transmit power level.

- Less CSHI: Schemes 2 and Scheme 4.
  1) According to Definition 4, the SALs of these two schemes approach but do not achieve the upper bound $\overline{\mathcal{A}}_{\mathrm{PU}}$, and gaps are -44.9485 dB and -10.9206 dB respectively.
  2) In Fig. 3(b), Schemes 2 and Scheme 4 encounter capacity floors stabilize at 0.4999 bit/s/Hz and 1.0666 bit/s/Hz respectively. The floors are caused by the interference of superposition coding, which prevent the SINR from continuously increasing with the increasing transmit power level.
  3) The observations of 2) exhibit that the two schemes are not CSHI-exempt. Whereas, the end-to-end capacity at "floors" is much higher than primary threshold $R_{th}=0.4$, which leads to relatively low error/outage probability. Thus, if the primary system has a low threshold R_{th}, it will be easy for none-CSHI-exempt schemes to approach the upper bound $\overline{\mathcal{A}}_{\mathrm{PU}}$ instead of achieving it.
- Severe CSHI: Scheme 3.
  1) The SAL of Scheme 3 stabilizes at 0.2588, which is far below $\overline{\mathcal{A}}_{\mathrm{PU}}=1$ in Table IV. A widening gap of

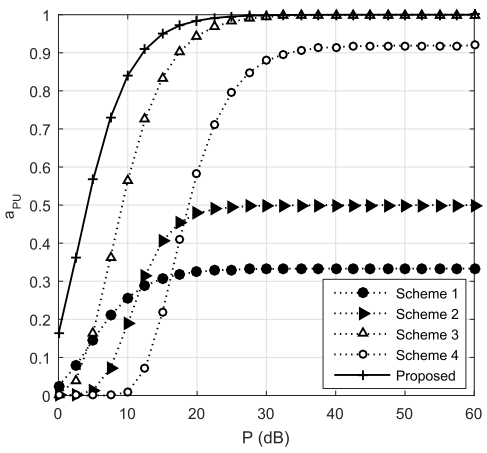

(a) a_{SU}

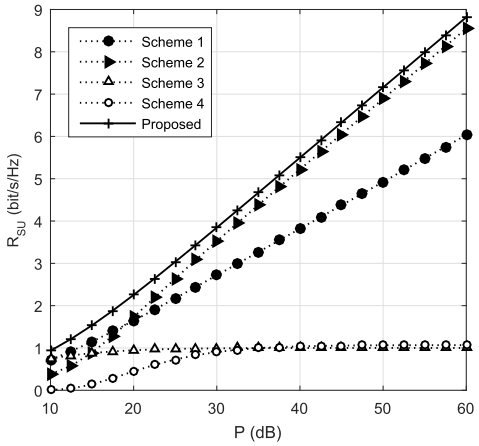

(b) R_{SU}

Fig. 4. Spectrum access level a_{PU} and end-to-end capacity R_{PU} of secondary system at different transmit power level.

-1.3006 dB exists between the maximal SAL and its upper bound.

2) The maximal primary end-to-end capacity of Scheme 3 is on a floor of 0.5570 bit/s/Hz, which is caused by the interference of superposition coding.
3) Although the capacity floor is much higher than R_{th}, the average one-way end-to-end capacity is $0.2785 < R_{th} = 0.4$. According to the definition of spectrum access level, the capacity of $link$ is 0.2785 bit/s/Hz which is far below threshold R_{th}. Thus, the probability of error/outage is rather high, and spectrum access level is below the upper bound $\overline{\mathcal{A}}_{\mathrm{PU}}$ at high SINR.

B. SALs and End-to-End Capacities of Secondary Systems

Fig. 4(a) and Fig. 4(b) compare different secondary systems in terms of SAL and end-to-end capacity. The detailed numerical results are presented in this section.

- CSHI-exempt: Scheme 1 and the proposed scheme.
  1) At high power level, the two schemes achieve their maximal SALs as $\frac{1}{3}$ and 1 (in Table IV) respectively, which are the upper bounds concerning their CSH models.
  2) The observation of 1) can be explained by the facts in Fig. 4(b), which exhibits no floors in the end-to-end capacity curves of these two schemes. As the power level is high enough, the SINR is $\gamma_{lilnk}(P) = \infty$, which satisfies Definition 3.
  3) It can be shown from Fig. 4(a) and 4(b) that the interference-free schemes can achieve the best distinguishable SAL performance for each of the two CSH systems.
- CSHI-exempt: Scheme 2
  1) The SAL of this scheme achieves the upper bound $\overline{\mathcal{A}}_{\mathrm{SU}} = 0.5$ (in Table IV) concerning its system model.
  2) The reachability of the upper bound $\overline{\mathcal{A}}_{\mathrm{SU}}$ can be explained by the fact that no floor appears in the end-to-end capacity curve of scheme 2. Due to the interference cancellation design of this scheme, SU decodes and regenerates the signal received in the first phase and cancels it from the interference signal superposed in the second phase, of which the success probability of decoding in the first phase increases simultaneously with the increasing transmit power level P. Thus, At high transmit power level, the SU's decoding can be viewed as interference-free. According to Definition 3, Scheme 2 can achieve the upper bound of the CSH system model.
  3) The results of scheme 2 verify that the scheme with good interference management can help to achieve the best distinguishable SAL performance of the CSH system model.
- Less CSHI: Schemes 3 and Scheme 4.
  1) The SALs of these two schemes approach but can not achieve the upper bound $\overline{\mathcal{A}}_{\mathrm{SU}}$ (in Table IV) concerning their system models, and gaps are -52.2185 dB and -12.8311 dB respectively.
  2) The observations in 1) can be explained by Fig. 4(b). The end-to-end capacities for Scheme 3 and Scheme 4 stabilize at 1 and 1.0667, respectively. These floors are caused by the interference of superposition coding, which prevent the SINR from continuously increasing with the increasing transmit power level.
  3) Obviously, Scheme 3 and Scheme 4 are none-CSHI-exempt. Whereas, the end-to-end capacities at floors are much higher than secondary threshold $R_{th} = 0.4$, which leads to relatively low error/outage probabilities. Thus, if the secondary system has a low threshold R_{th}, the none-CSHI-exempt scheme will closely approach the the upper bound $\overline{\mathcal{A}}_{\mathrm{SU}}$, but can not achieve it.

C. User Participation Levels for CSH Systems

We consider the upper bound of UPL for CSH model ($\mathcal{L}_*|_{\mathcal{P}_{\mathcal{R}_{link}=0}}$) and the maximal UPL for each specific scheme ($l_*|_{P\to\infty}$). In Fig. 5, the gap (defined in (11)) is given above the two bars for each scheme.

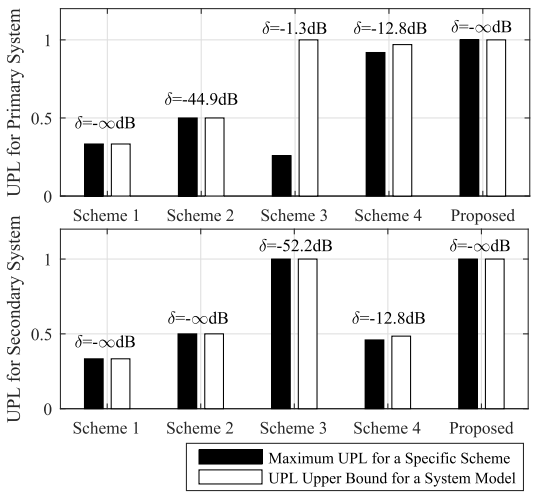

Fig. 5. The upper bound of UPL for CSH system model and maximal UPL for each scheme.

- As introduced in Definition 4, the gaps between $\mathcal{L}_*|_{\mathcal{P}_{\mathcal{R}_{link}}=0}$ and $l_*|_{P\to\infty}$ can reflect the efficiency of interference management for each scheme. Due to the potential relation of SAL to UPL, the explanation of these gaps are the same with analyses in the previous subsections and is omitted here.
- Both the proposed CSH system model and the supporting interference-free scheme can achieve the highest UPL amongst the comparing system models and schemes. No gap exists between $\mathcal{L}_*|_{\mathcal{P}_{\mathcal{R}_{link}}=0}$ and $l_*|_{P\to\infty}$.
- The upper bound of UPL for CSH system model ($\mathcal{L}_*|_{\mathcal{P}_{\mathcal{R}_{link}}=0}$) is the ideal maximal multiplexing gain for a CSH system, and $l_*|_{P\to\infty}$ is the actual maximal multiplexing gain a CSH scheme can achieve concerning interference.
- Some interesting observations and conclusions can be found via combining the numerical results of SAL and UPL.
  1) By jointly observing the primary SAL and UPL performances in Fig. 3(a) and Fig. 5, we can see that the previous gap in SAL between Scheme 4 and the proposed scheme is narrowed in the performance results of UPL. However, by jointly observing the secondary SAL and UPL performances in Fig. 4(a) and Fig. 5, we can see that the previous gap in SAL between Scheme 4 and the proposed scheme is widened in the performance results of UPL.
  2) These phenomena are closely related to the user capacities in Table III, which means less primary users in Scheme 4 can access the spectrum than that in the proposed scheme, while more secondary users in Scheme 4 can access the spectrum than that in the proposed scheme. As the number of PUs to access the spectrum in Scheme 4 is half of the proposed scheme, the sum spectrum access ability (revealed by SAL) has no superiority to it. Whereas, thanks to the good spectrum access ability of a individual PU (revealed by UPL), the gap can be narrowed. The widened gap in UPL can be similarly explained as the analyses above.

VI. Conclusions

In this paper, SAL and UPL metrics have been proposed to quantify the spectrum access ability for cooperative spectrum harvesting. The SAL metric measures how efficiently the spectrum is utilized by all considered users and can reveal the spectrum access efficiency. The UPL metric reflects the spectrum access ability of an individual user and can reveal the multiplexing gain. The proposed metrics have distinguishable upper bounds as SINR approaches infinity, and have advantage of being evaluated directly by CSH model. Using the SAL and UPL metrics, we have proposed a novel CSH model with an CSHI-exempt scheme, which aims to fully exploit the spectrum access ability. Through performance analysis, we can see the proposed system model with CSHI-exempt scheme has high SAL and UPL, and can also achieve the upper bounds of these two metrics. Through numerical results, on one hand, we have verified the efficiency of proposed metrics and the good spectrum access ability of proposed system. On the other hand, the SAL and UPL of existing CSH models have been presented, and we have exploited the causations of performance gaps and differences. In addition, we have shown that SAL has relation with UPL in definition, but UPL also depends highly on user capacity of CSH model.

References

[1] G. Wang, Q. Liu, R. He, F. Gao, and C. Tellambura, "Acquisition of channel state information in heterogeneous cloud radio access networks: Challenges and research directions," *IEEE Wireless Commun.*, vol. 22, no. 3, pp. 100–107, Jun. 2015.

[2] H.-M. Wang, K.-W. Huang, Q. Yang, and Z. Han, "Joint source-relay secure precoding for MIMO relay networks with direct links," *IEEE Trans. Commun.*, vol. 65, no. 7, pp. 2781–2793, Jul. 2017.

[3] N. Ansari and T. Han, *Green Mobile Networks: A Networking Perspective*. Hoboken, NJ, USA: Wiley, 2016, p. 328. [Online]. Available: https://ieeexplore.ieee.org/xpl/bkabstractplus.jsp?bkn=7906175

[4] N. Ansari and T. Han, "Freenet: Spectrum and energy harvesting wireless networks," *IEEE Netw.*, vol. 30, no. 1, pp. 66–71, Jan./Feb. 2016.

[5] Y. Liu, Y. Zhang, R. Yu, and S. Xie, "Integrated energy and spectrum harvesting for 5G wireless communications," *IEEE Netw.*, vol. 29, no. 3, pp. 75–81, May/Jun. 2015.

[6] N. Zhang, H. Zhou, K. Zheng, N. Cheng, J. W. Mark, and X. Shen, "Cooperative heterogeneous framework for spectrum harvesting in cognitive cellular network," *IEEE Commun. Mag.*, vol. 53, no. 5, pp. 60–67, May 2015.

[7] J. C. F. Li, W. Zhang, A. Nosratinia, and J. Yuan, "SHARP: Spectrum harvesting with ARQ retransmission and probing in cognitive radio," *IEEE Trans. Commun.*, vol. 61, no. 3, pp. 951–960, Mar. 2013.

[8] M. Pan, C. Zhang, P. Li, and Y. Fang, "Spectrum harvesting and sharing in multi-hop CRNs under uncertain spectrum supply," *IEEE J. Sel. Areas Commun.*, vol. 30, no. 2, pp. 369–378, Feb. 2012.

[9] D. Niyato and E. Hossain, "Spectrum trading in cognitive radio networks: A market-equilibrium-based approach," *IEEE Wireless Commun.*, vol. 15, no. 6, pp. 71–80, Dec. 2008.

[10] C. Jiang, L. Duan, and J. Huang, "Optimal pricing and admission control for heterogeneous secondary users," *IEEE Trans. Wireless Commun.*, vol. 15, no. 8, pp. 5218–5230, Aug. 2016.

[11] L. Gao, L. Duan, and J. Huang, "Two-sided matching based cooperative spectrum sharing," *IEEE Trans. Mobile Comput.*, vol. 16, no. 2, pp. 538–551, Feb. 2017.

[12] N. Zhang, H. Zhou, K. Zheng, N. Cheng, J. W. Mark, and X. Shen, "Cooperative heterogeneous framework for spectrum harvesting in cognitive cellular network," *IEEE Commun. Mag.*, vol. 53, no. 5, pp. 60–67, May 2015.

[13] A. Goldsmith, S. A. Jafar, I. Maric, and S. Srinivasa, "Breaking spectrum gridlock with cognitive radios: An information theoretic perspective," *Proc. IEEE*, vol. 97, no. 5, pp. 894–914, May 2009.
[14] Y. Cao and C. Tellambura, "Joint distributed beamforming and power allocation in underlay cognitive two-way relay links using second-order channel statistics," *IEEE Trans. Signal Process.*, vol. 62, no. 22, pp. 5950–5961, Nov. 2014.
[15] N. Devroye, P. Mitran, and V. Tarokh, "Achievable rates in cognitive radio channels," *IEEE Trans. Inf. Theory*, vol. 52, no. 5, pp. 1813–1827, May 2006.
[16] N. Devroye, P. Mitran, and V. Tarokh, "Limits on communications in a cognitive radio channel," *IEEE Commun. Mag.*, vol. 44, no. 6, pp. 44–49, Jun. 2006.
[17] C. Zhai, W. Zhang, and P. C. Ching, "Cooperative spectrum sharing based on two-path successive relaying," *IEEE Trans. Commun.*, vol. 61, no. 6, pp. 2260–2270, Jun. 2013.
[18] Y. Pei and Y.-C. Liang, "Cooperative spectrum sharing with bidirectional secondary transmissions," *IEEE Trans. Veh. Technol.*, vol. 64, no. 1, pp. 108–117, Jan. 2015.
[19] C. Ma, G. Sun, X. Tian, K. Ying, H. Yu, and X. Wang, "Cooperative relaying schemes for device-to-device communication underlaying cellular networks," in *Proc. IEEE GLOBECOM*, Dec. 2013, pp. 3890–3895.
[20] Y. Pei and Y.-C. Liang, "Resource allocation for device-to-device communications overlaying two-way cellular networks," *IEEE Trans. Wireless Commun.*, vol. 12, no. 7, pp. 3611–3621, Jul. 2013.
[21] L. Sun, Q. Du, P. Ren, and Y. Wang, "Two birds with one stone: Towards secure and interference-free D2D transmissions via constellation rotation," *IEEE Trans. Veh. Technol.*, vol. 65, no. 10, pp. 8767–8774, Oct. 2016.
[22] G. Zhang, K. Yang, P. Liu, and J. Wei, "Power allocation for full-duplex relaying-based D2D communication underlaying cellular networks," *IEEE Trans. Veh. Technol.*, vol. 64, no. 10, pp. 4911–4916, Oct. 2015.
[23] H. Gao, W. Ejaz, and M. Jo, "Cooperative wireless energy harvesting and spectrum sharing in 5G networks," *IEEE Access*, vol. 4, pp. 3647–3658, 2016.
[24] D. Zhang, R. Shinkuma, and N. B. Mandayam, "Bandwidth exchange: An energy conserving incentive mechanism for cooperation," *IEEE Trans. Wireless Commun.*, vol. 9, no. 6, pp. 2055–2065, Jun. 2010.
[25] H.-M. Wang, "Full-diversity uncoordinated cooperative transmission for asynchronous relay networks," *IEEE Trans. Veh. Technol.*, vol. 66, no. 1, pp. 468–480, Jan. 2017.
[26] L. Duan, L. Gao, and J. Huang, "Cooperative spectrum sharing: A contract-based approach," *IEEE Trans. Mobile Comput.*, vol. 13, no. 1, pp. 174–187, Jan. 2014.
[27] A. Gupta and R. K. Jha, "A survey of 5G network: Architecture and emerging technologies," *IEEE Access*, vol. 3, pp. 1206–1232, 2015.
[28] T. H. Cormen, C. E. Leiserson, R. L. Rivest, and C. Stein, *Introduction to Algorithms*. Cambridge, MA, USA: MIT Press, 2001.
[29] L. Yang, J. Chen, Y. Kuo, and H. Zhang, "Outage performance of DF-based cooperative multicast in spectrum-sharing cognitive relay networks," *IEEE Commun. Lett.*, vol. 18, no. 7, pp. 1250–1253, Jul. 2014.
[30] L. Zheng and D. N. C. Tse, "Diversity and multiplexing: A fundamental tradeoff in multiple-antenna channels," *IEEE Trans. Inf. Theory*, vol. 49, no. 5, pp. 1073–1096, May 2003.
[31] P. Gupta and P. R. Kumar, "The capacity of wireless networks," *IEEE Trans. Inf. Theory*, vol. 46, no. 2, pp. 388–404, Mar. 2000.
[32] S. P. Weber, X. Yang, J. G. Andrews, and G. de Veciana, "Transmission capacity of wireless ad hoc networks with outage constraints," *IEEE Trans. Inf. Theory*, vol. 51, no. 12, pp. 4091–4102, Dec. 2005.
[33] J. G. Andrews, S. Weber, M. Kountouris, and M. Haenggi, "Random access transport capacity," *IEEE Trans. Wireless Commun.*, vol. 9, no. 6, pp. 2101–2111, Jun. 2010.
[34] M. Ji, G. Caire, and A. F. Molisch, "Wireless device-to-device caching networks: Basic principles and system performance," *IEEE J. Sel. Areas Commun.*, vol. 34, no. 1, pp. 176–189, Jan. 2016.
[35] F. M. J. Willems, "The discrete memoryless multiple access channel with partially cooperating encoders (Corresp.)," *IEEE Trans. Inf. Theory*, vol. IT-29, no. 3, pp. 441–445, May 1983.
[36] J. Du, M. Xiao, M. Skoglund, and M. Médard, "Wireless multicast relay networks with limited-rate source-conferencing," *IEEE J. Sel. Areas Commun.*, vol. 31, no. 8, pp. 1390–1401, Aug. 2013.
[37] L. Sun, T. Zhang, and H. Niu, "Inter-relay interference in two-path digital relaying systems: Detrimental or beneficial?" *IEEE Trans. Wireless Commun.*, vol. 10, no. 8, pp. 2468–2473, Aug. 2011.
[38] M. Klugel and W. Kellerer, "Introduction of an efficiency metric for device-to-device communication in cellular networks," in *Proc. IEEE 80th Veh. Technol. Conf.*, Sep. 2014, pp. 1–6.
[39] Y. Fan, C. Wang, J. Thompson, and H. V. Poor, "Recovering multiplexing loss through successive relaying using repetition coding," *IEEE Trans. Wireless Commun.*, vol. 6, no. 12, pp. 4484–4493, Dec. 2007.
[40] N. Li, Y. Li, T. Wang, M. Peng, and W. Wang, "Full-duplex based spectrum sharing in cognitive two-way relay networks," in *Proc. IEEE PIMRC*, Aug./Sep. 2015, pp. 997–1001.

Chao Ren (S'15–M'18) received the B.Eng. degree from the Ocean University of China in 2011 and the Ph.D. degree from Xidian University in 2017. From 2015 to 2017, he was a Joint Ph.D. Student with the University of Alberta, Canada, sponsored by the China Scholarship Council. He is currently a Lecturer with the University of Science and Technology Beijing, China. His current research interests include cognitive radio, cooperative networks, device-to-device communications, edge computing, and full-duplex relaying. He served as a Technical Program Committee Member for IEEE VTC 2017, IEEE VTC 2018, and ICC 2019.

Haijun Zhang (M'13–SM'17) was a Post-Doctoral Research Fellow with the Department of Electrical and Computer Engineering, The University of British Columbia, Vancouver Campus, Canada. He is currently a Full Professor with the University of Science and Technology Beijing, China. He was a recipient of the IEEE CSIM Technical Committee Best Journal Paper Award in 2018 and IEEE ComSoc Young Author Best Paper Award in 2017. He serves as an Editor for the IEEE TRANSACTIONS ON COMMUNICATIONS, the IEEE TRANSACTIONS ON GREEN COMMUNICATIONS AND NETWORKING, and the IEEE 5G TECH FOCUS.

Jian Chen (M'14) received the B.Sc. degree from Xi'an Jiaotong University, China, in 1989, the M.S. degree from the Xi'an Institute of Optics and Precision Mechanics, Chinese Academy of Sciences, in 1992, and the Ph.D. degree in telecommunications engineering from Xidian University, Xi'an, China, in 2005. He was a Visiting Scholar with The University of Manchester from 2007 to 2008 and a Senior Visiting Scholar with the University of Alberta from 2017 to 2018. He is currently a Professor with the School of Telecommunications Engineering, Xidian University. His current research interests include cognitive radio, OFDM, wireless sensor networks, and non-orthogonal multiple access.

Chintha Tellambura (F'11) received the B.Sc. degree (Hons.) from the University of Moratuwa, Sri Lanka, the M.Sc. degree in electronics from the Kings College, University of London, U.K., and the Ph.D. degree in electrical engineering from the University of Victoria, Canada. He was with Monash University, Australia, from 1997 to 2002. He is currently a Professor with the Department of Electrical and Computer Engineering, University of Alberta. His current research interests include the design, modeling, and analysis of cognitive radio, heterogeneous cellular networks, 5G wireless networks, and machine learning algorithms.

He has authored or co-authored over 500 journal and conference papers with an h-index of 67 (Google Scholar). In 2017, he was elected a fellow of the Canadian Academy of Engineering. He received best paper awards in the Communication Theory Symposium at the 2012 IEEE International Conference on Communications (ICC) in Canada and the 2017 ICC in France. He was the Winner of the Prestigious McCalla Professorship and the Killam Annual Professorship from the University of Alberta. He served as an Editor for the IEEE TRANSACTIONS ON COMMUNICATIONS from 1999 to 2011 and the IEEE TRANSACTIONS ON WIRELESS COMMUNICATIONS from 2001 to 2007. He was an Area Editor for *Wireless Communications Systems and Theory* from 2007 to 2012.